

Dynamic FE Analysis of Ground Vibrations and Mitigation Measures for Stationary and Non-Stationary Transient Source

Lindita Kellezi

GEO – Danish Geotechnical Institute, Lyngby, Denmark

ABSTRACT: For building constructions located on soft soil conditions and near heavy traffic or industrial areas ground vibrations are becoming more and more a great concern. In this paper a three-dimensional (3D) finite element (FE) model formulation and its application for simulating ground vibration and design of mitigation measures is presented. The effectiveness of wave barriers such as concrete walls and a row of concrete piles in reducing those vibrations is investigated. The analyses consider stationary and non-stationary dynamic, transient sources intending to simulate industrial foundation vibrations and traffic-induced vibrations respectively. For non-stationary source subsonic conditions are considered. The far field is simulated by absorbing boundaries constructed based on the radiation criterion and strength of materials theory and considered as doubly asymptotic approximations. Numerical examples are presented which highlight the efficiency of the method in deriving useful engineering solutions assessing that a concrete wall might give up to 70% vibration reduction and a row of concrete pile up to 50 % reduction.

1 GENERAL INTRODUCTION

New infrastructure developments around the world are associated with an increased awareness regarding vibrations in buildings being an essential element in annoying people. Air borne noise is to an increasing extent being efficiently reduced by sound barriers, and the vibrations are remaining the dominant problem.

In different countries in Europe and elsewhere, official regulations have recently started focusing on limiting vibrations, setting up legal limits for acceptable levels.

Under these circumstances there is an increasing demand for better prediction methods regarding ground vibration, particularly for critical soil conditions involving soft soil layers at different depths. In addition, better tools for designing mitigation measures, which can reduce the through ground vibrations, are also required.

The predominant range of frequencies of such type of vibrations may be (5 - 50) Hz. The waves propagating at low frequency can interact with the modes of vibration of the nearby buildings, sometimes approaching resonance conditions, increasing the disturbance as schematized in Figure 1.

For heavy machineries operating in the industry or other similar situations the vibration source is considered fixed or stationary.

With the expansion of heavy traffic in the urban areas and railway network, concern has been raised about the effect of non-stationary load on wave propagation and vibrations in the nearby buildings.

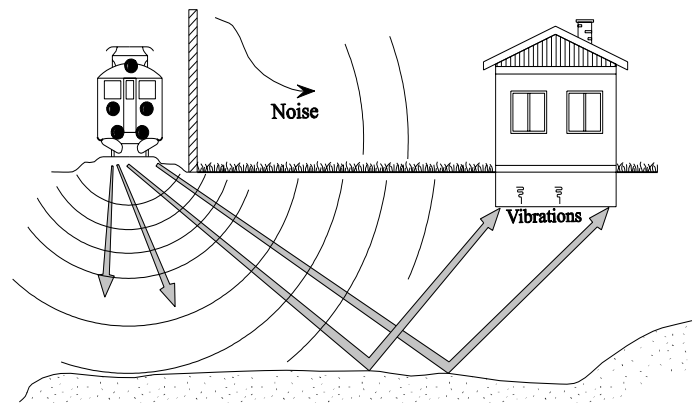


Figure 1. Noise and ground vibration transmission

Different vibration mitigation measures are proposed and applied in the past and recently. Open or in-filled trenches, concrete or sheet pile walls and wave impeding barriers have been previously investigated analytically and numerically by Ahmad et al, (1996), Al-Hussaini & Ahmad (1996), Hawwa (1998), Lee & Its (1995), Fuyuki & Matsumoto (1980), Takemiya & Kellezi (1998), Kellezi & Nielsen (2000) etc.

(Aviles & Sanchez-Sesma, (1988) investigated analytically a row of circular piles as ground vibra-

tion barrier. A general analytical solution was presented also from Boroomand & Kaynia (1991) considering dynamic pile-soil-pile-interaction. Kellezi & Foged (2001) investigated numerically different kinds of such barriers

3D FE modeling of the ground vibrations and mitigation measures, with special attention on concrete walls and row of concrete piles, which are possibly cheaper engineering solutions in practice, are presented in this paper. The analyses are carried out for stationary and non-stationary load assumptions

The description of the numerical method formulated, developed and applied in the analyses is given in the next section.

2 DEVELOPMENT OF 3D FE METHOD

2.1 Stationary Transient Source

When σ_{ij} and u_i denote the stress and displacement components respectively, ρ soil density and $p(t)$ the applied time function stress, the elasto-dynamic equations of motion are given as

$$\frac{\partial \sigma_{ij}}{\partial x_j} - \rho \frac{\partial^2 u_i}{\partial t^2} + p(t) = 0 \quad (1)$$

When Equations 1 are multiplied by a weight function in the form of a virtual displacement field u_i followed by integration over the volume and reformulation using the divergence theorem, Equation 2 is derived.

$$\int_{\Gamma} \bar{u}_i (\sigma_{ij} n_j) d\Gamma - \int_{\Omega} (\bar{\varepsilon}_{ij} \sigma_{ij} + \rho \bar{u} \ddot{u} - \bar{u} p) d\Omega = 0 \quad (2)$$

The stress σ_{ij} at the boundary integral in Equation 2 represent the stiffness of the far field and geometrical damping given in vector form in Equation 3.

$$\{\sigma\} = [D_K] \{u\} + [D_C] \{u_{,t}\} \quad (3)$$

The integral identity, Equation 2, reduces to a set of linear equations when the spatial variation of the actual and virtual displacement fields is represented by shape functions and Equation 3 is substituted. As a result the following equations of motions in matrix form derives

$$\begin{aligned} [M] \{u_{,tt}\} + ([C] + [C]_{\infty}) \{u_{,t}\} + \\ ([K] + [K]_{\infty}) \{u\} = \{P(t)\} \end{aligned} \quad (4)$$

$\{u\}$, $\{u_{,t}\}$ and $\{u_{,tt}\}$ are the system vectors for displacement, velocity and acceleration respectively. $[M]$ is the mass matrix. The system stiffness consists of the volume contribution $[K]$ and the stiffness arising from the integral over absorbing boundary $[K]_{\infty}$. The FE consistent stiffness at the boundary surface is derived as

$$[k]_{\infty} = \int_{\Gamma} [\bar{N}]^T [D_K] [\bar{N}] d\Gamma \quad (5)$$

The damping of the system consists of $[C]$ which models material damping for the near and the far field and the boundary integral, which models radiation damping $[C]_{\infty}$. Material damping matrix is constructed based on Raleigh damping. The FE consistent damping at the boundary surface derives as

$$[c]_{\infty} = \int_{\Gamma} [\bar{N}]^T [D_C] [\bar{N}] d\Gamma \quad (6)$$

The load vector $\{P(t)\}$ is the usual weighted integral of the surface traction. The matrices in Equation 5 and 6 are formulated in terms of the element shape function matrix, constitutive matrix for the far field stiffness $[D_K]$ and constitutive matrix for the far field geometrical or radiation damping $[D_C]$.

The formulation of the absorbing boundaries consist of how the constitutive matrices $[D_K]$ and $[D_C]$ are derived.

When an impulse is acting on an elastic half space medium in the 3D analysis, the surface at infinity for body waves is a large hemisphere with radius $r \rightarrow \infty$. For R-waves the surface at infinity is a flat cylinder with radius r and height approximately one R-wave length λ_R .

From the one-dimensional wave theory hemispherical P- or S wave fronts traveling in the positive z-direction could be closely approximated by

$$u_i(z, t) = \frac{1}{z} f(z - c_{P(S)} t) \quad (7)$$

For the conical horn, the differential equation of motion for a P or S wave reduces to

$$\frac{1}{c_{P(S)}} u_{i,tt} - \frac{2}{z} u_{i,z} - u_{i,zz} = 0 \quad (8)$$

Considering only outgoing waves given as in Equation 7 the boundary differential equation reduces to

$$\left[\frac{\partial}{\partial t} + \frac{c_{P(S)}}{z} + c_{P(S)} \frac{\partial}{\partial z} \right] u_i = 0 \quad (9)$$

The boundary stress at location z derives as

$$\sigma_i(x, t) = - \left[\frac{\rho c_{P(S)}^2}{z} u_i(z, t) + \rho c_{P(S)} u_{i,t}(z, t) \right] \quad (10)$$

The cones from the boundary location z to infinity are modeled by a mechanical system, which contains a spring and a damper with frequency independent coefficients.

From this investigation cone models are used as absorbing boundary for body waves in 3D FE dynamic analysis, They are applied for all degrees of

freedoms (DOF's) at the boundary defining the distance r of each Gauss integration point from the energy source, and knowing the coordinates of wave direction vectors \mathbf{r} and vectors \mathbf{n} normal to the boundary. Matrices $[D_K]$ and $[D_C]$ in Equations 3 and 5 and 6 derive as

$$[D_K] = \frac{\rho}{r} (n * r) \{c_p^2 [N] + c_s^2 ([I] - [N])\} \quad (11)$$

$$[D_C] = \rho (n * r) \{c_p [N] + c_s ([I] - [N])\} \quad (12)$$

Using Cartesian coordinates. $[I]$ is the identity matrix and $[N]$ is a 3×3 matrix. Its elements are products of coordinates of vectors \mathbf{n} (n_x, n_y, n_z).

So body waves in the 3D FE analysis are absorbed in the far field by a combination of cones simulated from springs and dashpots attached to the boundary nodes and connected to a rigid base. Apexes of the cones derive from the geometry of the model and source location.

Regarding surface waves, in the context of 1D wave theory a cylindrical wave traveling in the positive x -direction is approximated by

$$u_i(x, t) = \frac{1}{\sqrt{x}} f(x - ct) \quad (13)$$

For soil half space model $c=c_R$ for example for the horizontal component of the in-plane motion. From the strength of materials theory the differential equation satisfied from a cylindrical wave front could be

$$\frac{1}{c} u_{i,tt} - \frac{1}{x} u_{i,x} - u_{i,xx} = 0 \quad (14)$$

This is the equation of motion of a cone with linear area variation. Considering only outgoing waves the boundary differential equations equals

$$\left[\frac{\partial}{\partial t} + \frac{c}{2x} + c \frac{\partial}{\partial x} \right] u_i = 0 \quad (15)$$

The boundary stress derives as

$$\sigma_i(x, t) = - \left[\frac{\rho c^2}{2x} u_i(x, t) + \rho c u_{i,t}(x, t) \right] \quad (16)$$

The linear cones from the boundary location x to infinity are modeled also by a mechanical system, which contains a spring and a damper with frequency independent coefficients.

These models are used as absorbing boundary for surface waves in similar way as for the body waves with constitutive stiffness matrices $[D_K]$ and $[D_C]$ derived as

$$[D_K] = \frac{\rho}{r} (n * r) \left\{ \frac{1}{2} (sc_R^2 n_x^2 + c_R^2 (1 - n_z^2)) + c_s^2 n_y^2 \right\} \quad (17)$$

$$[D_C] = \rho (n * r) \{sc_R n_x^2 + c_R (1 - n_z^2) + c_s n_y^2\} \quad (18)$$

In Equations 17 and 18 s is the ratio of P- to S wave velocities.

Development of the above method in two-dimensional (2D), plane strain, and axisymmetric conditions is presented in Kellezi (2000). Some verifications for 3D conditions are given in Kellezi & Takemiya (2001).

2.2 Non-Stationary Transient Source

Several studies have been carried out on the linear dynamic response of continuous pavements subjected to non-stationary loads, Hardy & Cebon (1993), Kim & Roesset (1998), etc.

Alternatively, the problem was formulated for 2D FE applications, plane strain, by (Krenk et al, 1999) for transient source of vibrations directly in the time domain. That formulation is further developed and applied for the 3D case implementing modified absorbing boundary conditions.

The convected equations of motion are given from Equation 19.

$$\frac{\partial \sigma_{ij}}{\partial x_j} - \rho \frac{\partial^2 u_i}{\partial t^2} + 2V_y \frac{\partial u_i}{\partial x_j \partial t} - V_y^2 \frac{\partial^2 u_i}{\partial x_j \partial x_k} = p(t) \quad (19)$$

V_y denotes the velocity of the non-stationary load. The load is supposed to move in the y -direction.

In matrix form the equations of motion derive as in Equation 20 after multiplied by a weight function in the form of a virtual displacement field followed by integration over the volume and using the divergence theorem.

$$[M] \{u_{,tt}\} + ([C] + [C_V] + [C]_{\infty} + [C_V]_{\infty}) \{u_{,t}\} + ([K] + [K_V] + [K]_{\infty} + [K_V]_{\infty}) \{u\} = \{P(t)\} \quad (20)$$

The effect of convection is a nonsymmetrical term, containing mixed time and spatial derivatives, which for the element is given by Equation 21, and a symmetrical term, containing the second spatial derivatives, which for the element is given by Equation 22.

$$[c_V] = -2 \int_{\Omega} \left[\bar{N} \right]^T \rho V_y \left[\bar{N}_{,y} \right] d\Omega \quad (21)$$

$$[k_V] = - \int_{\Omega} \left[\bar{N}_{,y} \right]^T \rho V_y^2 \left[\bar{N}_{,y} \right] d\Omega \quad (22)$$

Equation 23 and 24 give the change in the radiation damping and far field stiffness at the lateral boundary perpendicular to the moving direction, because of the non-stationary load effect

$$[c_V]_{\infty} = -\int_{\Gamma} [\bar{N}]^T n \rho V_y [\bar{N}] d\Gamma \quad (23)$$

$$[k_V]_{\infty} = -\int_{\Gamma} [\bar{N}]^T n \rho V_y^2 [\bar{N}_{,y}] d\Gamma \quad (24)$$

These velocity dependant damping and stiffness will have negative values for $y>0$ and positive values for $y<0$.

A second order correction is implemented in the convected equations of motions, as the problem is not self-adjoint and Galerkin discretization is approximate. This is based on an alternative version of the Taylor-Galerkin approach for the spatial discretization, (Krenk et al, 1999).

The rest of the matrices in Equation 20 are as given in section 2.1

2.3 3D FE Method Implementation and Application

All the matrices given in sections 2.1 and 2.2 are implemented in the FE method building a program applicable for elasto-dynamic FE analyses. Direct time integration was applied to handle transient loads

For stationary source, by using symmetry conditions only a quarter of the model was investigated. However, for non-stationary source moving in the y-direction, half of the FE model was considered using the symmetry conditions along the y-direction.

The transient load, simulating a heavy vehicle or moving train, is simulated by a hammer impulse function with period $T = 0.1$ s, generating frequencies (0 - 20) Hz. This load, which applies at point (0,0,0), is supposed to move with velocity $V_y = (70 - 90)$ km/h considering heavy traffic or existing slow-running trains going through areas with soft soil profiles.

Homogeneous half space soil conditions are considered with shear wave velocity $c_s=120$ m/s, density $\rho=1800$ kg/m³, Poisson ratio $\nu=0.4$ and material damping coefficient $\gamma=5\%$.

The 3D FE Model in Cartesian coordinates covers a sufficient area in the x and y-direction. It goes deeply into the half space as well. 8-node isoparametric cubic FE is employed with dimensions $dx=dy=dz=\lambda_s/6=2$ m. Absorbing boundaries are implemented at the bottom and the sides of the model at a distance less than two λ_s from the source.

To see the non-stationary load effect compared to a stationary load, the vertical displacement component at the soil surface, $z=0$, is given in Figure 2. The load with amplitude $P=40$ kN is applied.

The change in the system behavior when the load is non-stationary in comparison when it is stationary can be noticed by comparing Figure 2a with 2b

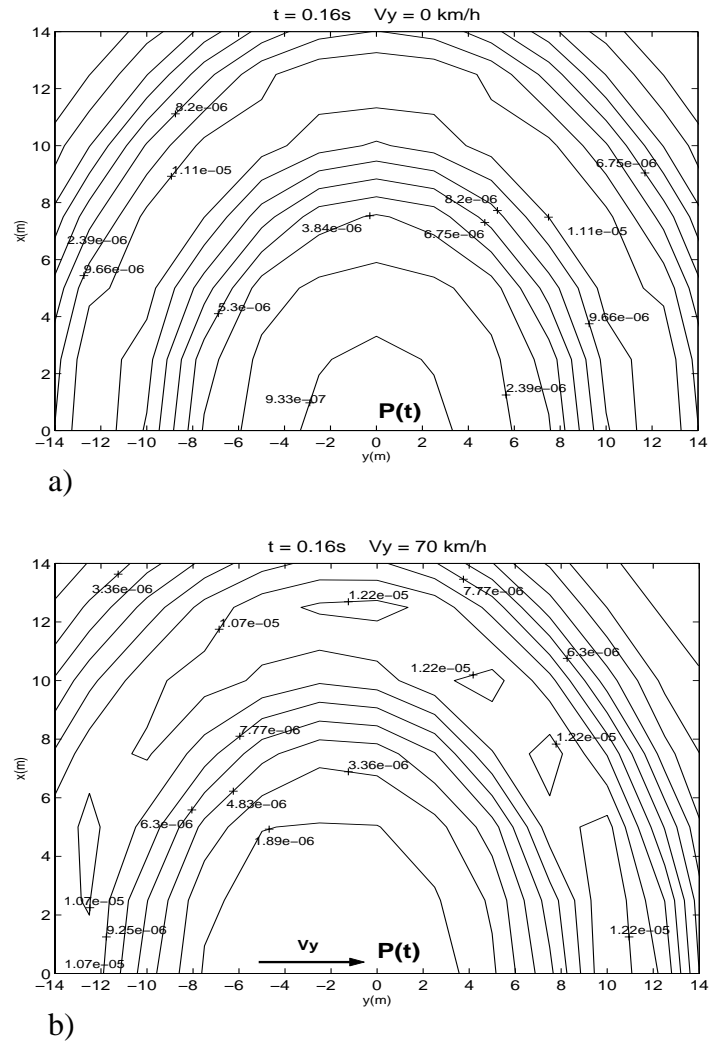


Figure 2. Vertical Displacement at $z=0$. a) Stationary load. b) Non-stationary load

For moving load the ground vibration amplitudes are different in the front and on the back of the load. The velocity of wave propagation in the soil will decrease in the moving direction and increase in the opposite direction.

3 GROUND VIBRATION MITIGATION MEASURES

Among other types of ground vibration mitigation measures, attention is given to the concrete walls and a row of concrete piles applied for stationary and non-stationary transient load conditions

3.1 Stationary Load

In Figure 3 parameters like R-the distance of the barrier from the source, L-half of the barrier length L_b , H-barrier depth and B-barrier width are noted. S-the net spacing between the piles for the row of piles is an important parameter as well.

$B=(0.03\div 0.04)\lambda_s$ is chosen considering the type of piles expected to be applied in Denmark.

For stationary load, $V_y=0$ there is symmetry in the x and y-direction. So a quarter of the model is considered. Computations given in Figure 4 and 5 are carried out varying the depth $h'=H/\lambda_s$ of the concrete wall and row of piles of cross section Bx4B and net spacing $S=4B$.

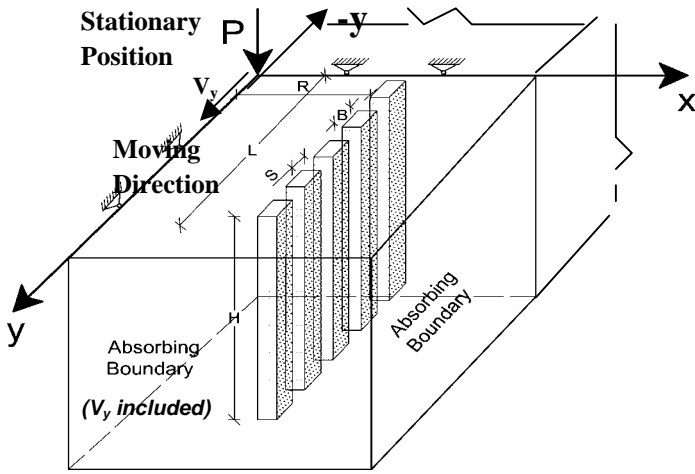


Figure 3. Solid wave barrier, row of concrete piles.

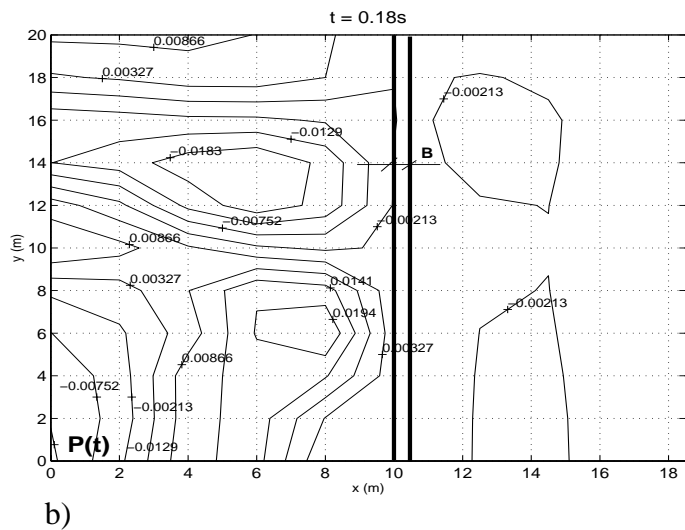
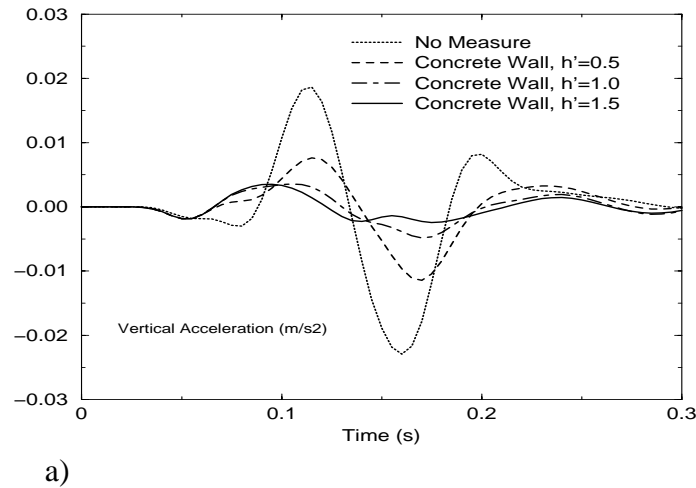


Figure 4. Concrete wall, Vertical Acceleration a) After the measure, at $x=12.5m$, $R=0.83\lambda_s$, $B=0.04\lambda_s$, $L=1.65\lambda_s$, b) At the soil surface, $R=0.83\lambda_s$, $B=0.04\lambda_s$, $L=1.65\lambda_s$, $h' = 1$

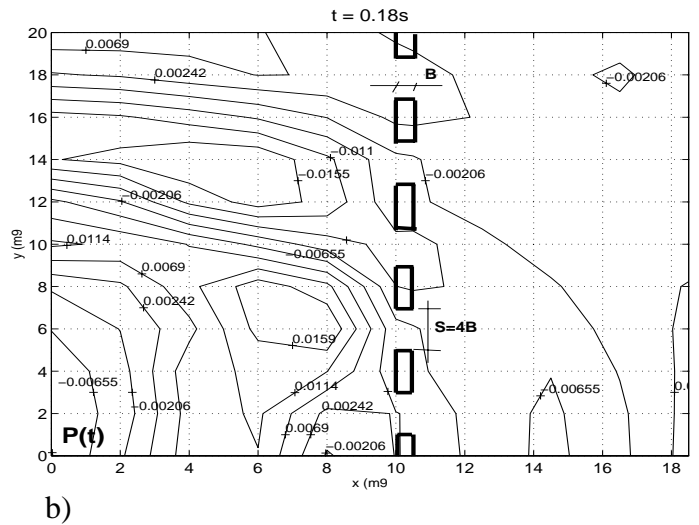
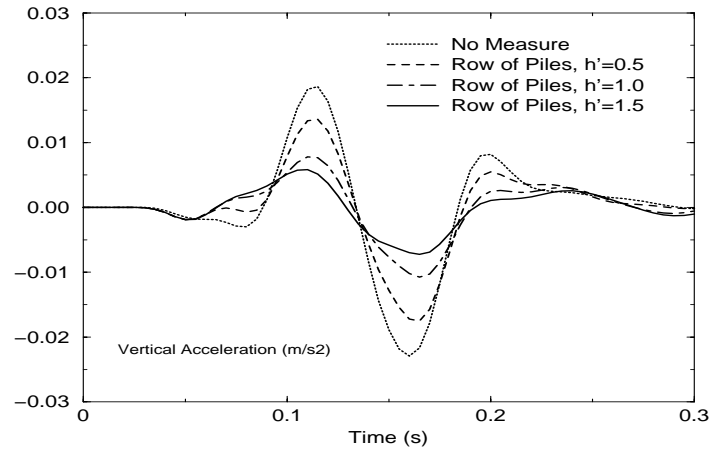


Figure 5 Row of concrete piles, Vertical Acceleration a) After the measure, at $x=12.5m$, $R=0.83\lambda_s$, $B=0.04\lambda_s$, $L=1.65\lambda_s$, b) At the soil surface, $R=0.83\lambda_s$, $B=0.04\lambda_s$, $L=1.65\lambda_s$, $h' = 1$

From Figure 4 and 5 we see that a concrete wall and a row of concrete sheet piles embedded in homogeneous soil conditions and designed as above, reduce the amplitude of ground vibrations at an amount (50 - 70)% and (30 - 50)% respectively for $h' = 0.5$ and $h' = 1.5$. This means that an amplitude reduction factor $A = (0.3 - 0.5)$ and $A = (0.5 - 0.7)$ or an isolation effectiveness $F = 1 - A = (0.5 - 0.7)$, and $F = (0.3 - 0.5)$ is achieved respectively at that location.

For the concrete wall as larger the width, larger the reduction capacity. When the wall is replaced with a row of concrete piles or sheet piles designed as in Figure 5 the reduction capacity drops, however considering the fact that construction work can be reduced and excavation work can be avoided, the profit is larger. On the other hand a row of piles can be constructed for areas below water table levels, which is not the case for a concrete wall.

The width B of the solid measures is an important parameter. Increasing B and decreasing the size of the net spacing S will increase the reduction capacity of the row of piles.

3.2 Non-stationary Load

As the intention is to use concrete ground vibration mitigation measures in the heavy traffic or running trains, it is interesting to see their effect in case of non-stationary vibration source. The parameters indicated in Figure 3 are still applicable but the moving load velocity is V_y .

In Figure 6a vertical displacement component is given when a concrete wall of width $B=1\text{m}$ is constructed and embedded in the ground. In Figure 6b the concrete wall is replaced by a row of concrete piles of dimensions $1\text{m}\times 2\text{m}$ placed at a distance $S=2B=2\text{m}$ from each other. The soil parameters are the same as for calculation carried out in section 2.3.

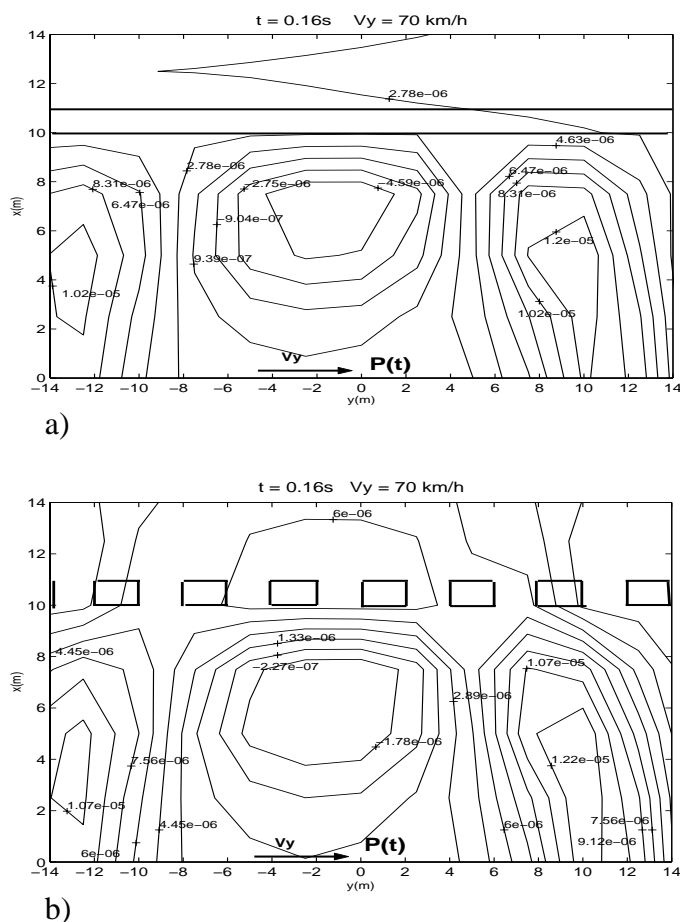


Figure 6. Vertical Displacement at the soil surface a) Concrete wall barrier, b) Row of Piles of $1\text{m}\times 2\text{m}$. $R=0.83\lambda_s$, $h'=1.5$, $L=1.5\lambda_s$, $B=0.08\lambda_s$, $S=0.17\lambda_s$.

4 CONCLUSIONS

3D FE analyses of ground vibrations and mitigation measures with emphasis on concrete walls and row of concrete piles were carried out in this paper. A 3D FEM program was formulated in Cartesian coordinates for stationary and non-stationary transient load.

To simulate unbounded soil domain, absorbing BC's were formulated and implemented at the boundaries of the FE model. For the frequency in-

terval and soil stiffness considered a concrete wall as wave barrier will give maximum (50 - 70)% ground vibration reduction and a dashed wall or a pile row with $S = 2B$ or $S = B$ will give (30 - 50)% reduction. The width of the barriers will determine the amount of reduction in the given intervals.

The method applies for the velocity of the non-stationary source smaller than the shear wave velocity of the ground, called subsonic conditions.

REFERENCES

- Ahmad, S. T.M., Al-Hussaini & K.L. Fishman, 1996. Investigation on Active Isolation of Machine Foundations by Open Trenches, *Journal of Geotechn. Eng.* 122(6), 454-461.
- Al-Hussaini, T.M. & Ahmad, S. 1996. Active Isolation of Machine Foundations by In-filled Trenches Barriers, *Journal of Geotech. Engrg.* Vol. 122(4), 288-294.
- Aviles, J. & Sanchez-Sesma, F.J. 1988. Foundation Isolation from Vibration Using Piles as Barriers. *Journal of Engrg. Mechanics*, Vol. 114(11), 1854-1870.
- Boroomand, B. & Kaynia, A. M. 1991. Vibration Isolation by an Array of Piles, *Soil Dyn. and Earthq. Engrg.* Ed IBF, Comp. Mech. Publicat. Elsevier Appl. Sc. 683-691.
- Fuyuki, M. & Matsumoto, Y. 1980. Finite Difference Analysis of Rayleigh Wave Scattering at a Trench, *Bulletin of Seism. Society of America*, Vol. 70(6), 2051-2069.
- Hardy, M.S.A, & Cebon, D. 1993. Response of Continuous Pavements to Moving Dynamic Loads, *Journal of Engrg. Mech.* Vol. 119, 1762-1780.
- Hawwa, A. Muhammad, 1998. Vibration Isolation of Machine Foundations by Periodic Trenches. *Journal of Engrg. Mech.* Vol. 124(4), 422-427.
- Lee, S.L. & Its, E. N. 1995. Surface Waves of Oblique Incidence Across Deep In-filled Trenches, *Journal of Engrg. Mech.* Vol. 12(3), 482-486.
- Kellezi, L. 2000, Transmitting Boundaries for Transient Elastic Analysis. *Journal of Soil Dynamics and Earthquake Engineering*. Vol. 19, No. 7, 533-547.
- Kellezi, L. & Nielsen, L. O. 2000. Dynamic Behaviour of a Soil Stratum and Vibration Reduction, *13th Nordic Geotech. Conf.* Helsinki, Proc. N99.
- Kellezi, L. & Takemiya, H. 2001. An Effective Local Absorbing Boundary for 3D FEM Time Domain Analyses, *4th Intern. Conf. on Recent Adv. on Geot. Earthq. Engrg. and Soil Dyn.* San Diego, Paper No 3.42.
- Kellezi, L. & Foged, N. 2001. 3D FEM Analysis of Ground Vibration Measures for Moving and Stationary Transient Source, *4th International Conf. on Recent Advances on Soil Dynamics and Earthquake Eng.* March, San Diego, Paper No. 6.49.
- Kim, S.M., & Roesset, J. M. 1998. Moving Loads on a Plate on Elastic Foundation. *Journal of Eng. Mechanics*. Vol. 124, 1010-1017.
- Krenk, S., Kellezi, L., Nielsen, S. R. K., & Kirkegaard, P. H. 1999. Finite Elements and Transmitting Boundary Conditions for Moving Loads, *4th European Conf. on Structural Dynamics, Eurodyn'99*, Prague, Proc. Vol. 1, 447-452.
- Takemiya, H. & Kellezi, L. 1998. Paraseismic Behaviour of Wave Impeding Block (WIB) Measured for Ground Vibration Reduction, *10th Japan Earthquake Eng. Symposium*, Yokohama, E3-13, 1879-1884.